We are IntechOpen,
the world's leading publisher of
Open Access books
Built by scientists, for scientists

6,900
Open access books available

186,000
International authors and editors

200M
Downloads

Our authors are among the

154
Countries delivered to

TOP 1%
most cited scientists

12.2%
Contributors from top 500 universities

CLARIVATE ANALYTICS

BOOK CITATION INDEX

INDEXED

WEB OF SCIENCE™

Selection of our books indexed in the Book Citation Index
in Web of Science™ Core Collection (BKCI)

Interested in publishing with us?
Contact book.department@intechopen.com

Robust Control of the Two-mass Drive System Using Model Predictive Control

Krzysztof Szabat, Teresa Orłowska-Kowalska and Piotr Serkies
Wroclaw University of Technology
Poland

1. Introduction

A demand for the miniaturization and reducing the total moment of inertia which allows to shorten the response time of the whole system is evident in modern drives system. However, reducing the size of the mechanical elements may result in disclosure of the finite stiffness of the drive shaft, which can lead to the occurrence of torsional vibrations. This problem is common in rolling-mill drives, belt-conveyors, paper machines, robotic-arm drives including space manipulators, servo-drives and throttle systems (Itoh et al., 2004, Hace et al., 2005 , Ferretti et al. 2005, Sugiura & Hori, Y., 1996, Szabat & Orłowska-Kowalska, 2007, O'Sullivan at al. 2007, Ryvkin et al., 2003 , Wang & Frayman, 2004, Vasak & Peric, 2009, Vukosovic & Stojic, 1998).

To improve performances of the classical control structure with the PI controller, the additional feedback loop from one selected mechanical state variable can be used. The additional feedback allows setting the desired value of the damping coefficient, but the free value of the resonant frequency cannot be achieved simultaneously (Szabat & Orłowska-Kowalska, 2007). According to the literature, the application of the additional feedback from the shaft torque is very common (Szabat & Orłowska-Kowalska, 2007). The design methodology of that system can be divided into two groups. In the first framework the shaft torque is treated as the disturbance. The simplest approach relies on feeding back the estimated shaft torque to the control structure, with the gain less than one. The more advanced methodology, called Resonance Ratio Control (RRC) is presented in (Hori et al., 1999). The system is said to have good damping ability when the ratio of the resonant to antiresonant frequency has a relatively big value (about 2). The second framework consists in the application of the modal theory. Parameters of the control structure are calculated by comparison of the characteristic equation of the whole system to the desired polynomial. To obtain a free design of the control structure parameters, i.e. the resonant frequency and the damping coefficient, the application of two feedbacks from different groups of mechanical state variables is necessary. The design methodology of this type of the systems is presented in (Szabat & Orłowska-Kowalska, 2007).

The control structures presented so far are based on the classical cascade compensation schemes. Since the early 1960s a completely different approach to the analysis of the system dynamics has been developed – the state space methodology (Michels et al., 2006). The application of the state-space controller allows to place the system poles in an arbitrary position so theoretically it is possible to obtain any dynamic response of the system. The

suitable location of the closed-loop system poles becomes one of the basic problems of the state space controller application. In (Ji & Sul,, 1995) the selection of the system poles is realized through LQ approach. The authors emphasize the difficulty of the matrices selection in the case of the system parameter variation. The influence of the closed-loop location on the dynamic characteristics of the two-mass system is analyzed in (Qiao et al., 2002), (Suh et al., 2001). In (Suh et al., 2001) it is stated that the location of the system poles in the real axes improve the performance of the drive system and makes it more robust against the parameter changes.

In the case of the system with changeable parameters more advanced control concepts have been developed. In (Gu et al., 2005), (Itoh et al., 2004) the applications of the robust control theory based on the H_∞ and $\mu\text{-synthesis}$ frameworks are presented. The implementation of the genetic algorithm to setting of the control structure parameters is shown in (Itoh et al., 2004). The author reports good performance of the system despite the variation of the inertia of the load machine. The next approach consists in the application of the sliding-mode controller. For example, in paper (Erbatur et al., 1999) this method is applied to controlling the SCARA robot. A design of the control structure is based on the Lyapunov function. The similar approach is used in (Hace et al., 2005) where the conveyer drive is modelled as the two-mass system. The authors claim that the designed structure is robust to the parameter changes of the drive and external disturbances. Other application examples of the sliding-mode control can be found in (Erenturk, 2008). The next two frameworks of control approach relies on the use of the adaptive control structure. In the first framework the controller parameters are adjusted on-line on the basis of the actual measurements. For instance in (Wang & Frayman, 2004) a dynamically generated fuzzy-neural network is used to damp torsional vibrations of the rolling-mill drive. In (Orlowska-Kowalska & Szabat, 2008) two neuro-fuzzy structures working in the MRAS structure are compared. The experimental results show the robustness of the proposed concept against plant parameter variations. In the other framework changeable parameters of the plant are identified and then the controller is retuned in accordance with the currently identified parameters. The Kalman filter is applied in order to identify the changeable value of the inertia of the load machine (Szabat & Orlowska-Kowalska, 2008). This value is used to correct the parameters of the PI controller and two additional feedbacks. A similar approach is presented in (Hirovonen et al., 2006).

The Model Predictive Control (MPC) is one of the few techniques (apart from PI/PID techniques) which are frequently applied to industry (Maciejowski 2002, Cychowski 2009). The MPC algorithm adapts to the current operation point of the process generating an optimal control signal. It is able to directly take into consideration the input and output constraints of the system which is not easy in a control structure using classical structures. Nevertheless, the real time implementations of the MPC are traditionally limited to objects with relatively large time constants (Maciejowski 2002, Cychowski 2009). The application of MPC to industrial processes characterized by fast dynamics, such as those of electrical drives, is complicated by the formidable real-time computational complexity often necessitating the use of high-performance computers and complex software. The state-of-the-art of currently employed predictive control methods in the power electronics and motion control sector is given in (Kennel et al, 2008). Still, there are few works which report the application of the MPC in the control structure of a two-mass system (Cychowski et al. 2009).

The main contribution of this paper is the design and real-time validation of an explicit model predictive controller for a two-mass elastic drive system which is robust to the parameter changes. The explicit version of the MPC algorithm presented here does not involve complex optimization to be performed in a control unit but requires only a piecewise linear function evaluation which can be realized through a simple look-up table approach. This problem is computationally far more attractive than the standard optimization-based MPC and enables the application of complex constrained control algorithms to demanding systems with sampling in the mili/micro second scale. In addition to low complexity, the proposed MPC controller respects the inherent electromagnetic (input) and shaft (output) torque constraints while guaranteeing optimal closed-loop performance. This safety feature is crucial for many two-mass drive applications as violating the shaft ultimate tensile strength may result in damage of the shaft and ultimately in the failure of the entire drive system. Contrary to the previous works of the authors (Cychowski et al. 2009), where the system was working under nominal condition, in the present paper the issues related to the robust control of the drive system with elastic joint are presented.

This paper is divided into seven sections. After an introduction, the mathematical model of the two-mass drive system and utilized control structure are described. In section III the idea of the MPC is presented. Then the whole investigated control structure is described. The simulation results are demonstrated in sections V. After a short description of the laboratory set-up, the experimental results are presented in section VI. Conclusions are presented at the end of the paper.

2. The mathematical model of the two-mass system and the control structure

In technical papers there exist many mathematical models, which can be used for the analysis of the plant with elastic couplings. In many cases the drive system can be modelled as a two-mass system, where the first mass represents the moment of inertia of the drive and the second mass refers to the moment of inertia of the load side. The mechanical coupling is treated as an inertia free. The internal damping of the shaft is sometimes also taken into consideration. Such a system is described by the following state equation (Szabat & Orlowska-Kowalska, 2007) (with non-linear friction neglected):

$$
\frac{d}{dt}\begin{bmatrix} \Omega_1(t) \\ \Omega_2(t) \\ M_s(t) \end{bmatrix} = \begin{bmatrix} \dfrac{-D}{J_1} & \dfrac{D}{J_1} & \dfrac{-1}{J_1} \\ \dfrac{D}{J_2} & \dfrac{-D}{J_2} & \dfrac{1}{J_2} \\ K_c & -K_c & 0 \end{bmatrix} \begin{bmatrix} \Omega_1(t) \\ \Omega_2(t) \\ M_s(t) \end{bmatrix} + \begin{bmatrix} \dfrac{1}{J_1} \\ 0 \\ 0 \end{bmatrix} [M_e] + \begin{bmatrix} 0 \\ \dfrac{-1}{J_2} \\ 0 \end{bmatrix} [M_L] \tag{1}
$$

where: Ω_1- motor speed, Ω_2- load speed, M_e– motor torque, M_s– shaft (torsional) torque, M_L– load torque, J_1 – inertia of the motor, J_2– inertia of the load machine, K_c– stiffness coefficient, D – internal damping of the shaft.

The schematic diagram of the two-mass system is presented in Fig. 1

The described model is valid for the system in which the moment of inertia of the shaft is much smaller than the moment of the inertia of the motor and the load side. In other cases a more extended model should be used, such as the Rayleigh model of the elastic coupling or even a model with distributed parameters. The suitable choice of the mathematical model is

a compromise between the accuracy and calculation complexity. As can be concluded from the literature, nearly in all cases the simplest shaft-inertia-free model has been used.
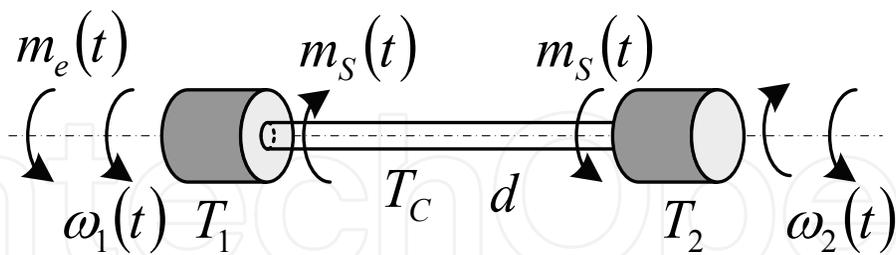

Fig. 1. The schematic diagram of the two-mass system

To simplify the comparison of the dynamical performances of the drive systems of different power, the mathematical model (1) is expressed in per unit system, using the following notation of new state variables:

$$\omega_1 = \frac{\Omega_1}{\Omega_N} \quad \omega_2 = \frac{\Omega_2}{\Omega_N} \quad m_e = \frac{M_e}{M_N} \quad m_s = \frac{M_s}{M_N} \quad m_L = \frac{M_L}{M_N} \tag{2}$$

where: Ω_N – nominal speed of the motor, M_N – nominal torque of the motor, ω_1, ω_2 – motor and load speeds, m_e, m_s, m_L – electromagnetic, shaft and load torques in per unit system.
The mechanical time constant of the motor – T_1 and the load machine – T_2 are thus given as:

$$T_1 = \frac{\Omega_N J_1}{M_N} \quad T_2 = \frac{\Omega_N J_2}{M_N} \tag{3}$$

The stiffness time constant – T_c and internal damping of the shaft – d can be calculated as follows:

$$T_c = \frac{M_N}{K_c \Omega_N} \quad d = \frac{\Omega_N D}{M_N} \tag{4}$$

Taking into account the equations (3)-(5) the state equation of the two-mass system in per-unit value is represented as:

$$\frac{d}{dt} \begin{bmatrix} \omega_1(t) \\ \omega_2(t) \\ m_s(t) \end{bmatrix} = \begin{bmatrix} 0 & 0 & \frac{-1}{T_1} \\ 0 & 0 & \frac{1}{T_2} \\ \frac{1}{T_c} & \frac{-1}{T_c} & 0 \end{bmatrix} \cdot \begin{bmatrix} \omega_1(t) \\ \omega_2(t) \\ m_s(t) \end{bmatrix} + \begin{bmatrix} \frac{1}{T_1} \\ 0 \\ 0 \end{bmatrix} \cdot m_e(t) + \begin{bmatrix} 0 \\ -\frac{1}{T_2} \\ 0 \end{bmatrix} \cdot m_L(t)$$

$$\frac{d}{dt} x_c = A_c x_c + B_c m_e + B_d m_L \tag{5}$$

Usually, due to its small value the internal damping of the shaft d is neglected in the analysis of the two-mass drive system as in eq. (5).

3. Model predictive control and its explicit formulation

In model predictive control, an explicit model of the plant is used to predict the effect of future actions of the manipulated variables on the process output. In the recent literature, the following linear discrete-time state-space model is typically employed [14]

$$x(k+1) = Ax(k) + Bu(k)$$
$$y(k) = Cx(k) \tag{6}$$

where $x(k)$, $u(k)$ and $y(k)$ denote the system state, input and output vectors, respectively. Let y_k represent the value of the output vector at a future time k, given an input sequence u_k, and initial state x_0 of the system. At each time step k, the MPC algorithm solves the following optimization problem:

$$\min_{u_0,...,u_{N_c-1}} \sum_{k=0}^{N_p} y_k^T \mathbf{Q} y_k + \sum_{k=0}^{N_c-1} u_k^T \mathbf{R} u_k$$

subject to

$$u_{\min} \leq u_k \leq u_{\max}, \quad k = 0,...,N_c - 1$$
$$y_{\min} \leq y_k \leq y_{\max}, \quad k = 1,...,N_p$$
$$x_{k+1} = Ax_k + Bu_k, \quad k \geq 0 \tag{7}$$
$$y_k = Cx_k, \qquad\qquad k \geq 0$$
$$x_0 = x(0)$$

where $Q \geq 0$ and $R > 0$ are the weighting matrices, N_p and N_c denote the prediction and control horizon, respectively and $u_{\min}$, $u_{\max}$, $y_{\min}$, and $y_{\max}$ are the input and output constraints of the system.

The MPC algorithm based on optimization problem can be implemented in two ways. The traditional approach relies on solving the optimization problem on-line for a given $x(k)$ in a receding-horizon fashion. This means that, at the current time k, only the first element control signal u_k of the optimal input sequence is actually implemented to the plant and the rest of the control moves are discarded. At the next time step, the whole procedure is repeated for the new measured or estimated output $y(k+1)$ (Maciejowski 2002, Cychowski 2009). This strategy can be computationally demanding for systems requiring fast sampling or low-performance computers and hence greatly restricting the scope of applicability to systems with relatively slow dynamics. In the second approach, the problem (7) is first solved off-line for all possible state realizations within some compact set X_f using multi-parametric programming (Maciejowski 2002, Cychowski 2009). Specifically, by treating the state vector $x(k)$ as a parameter vector, it can be shown that the parameter space X_f can be subdivided into characteristic regions, where the optimizer is given as an explicit function of the parameters. This profile is a piecewise affine state feedback law:

$$U(x) = K_r x + g_r, \quad \forall x \in P_r \tag{8}$$

where P_r are polyhedral sets defined as:

$$P_r = \left\{ x \in \Re^n \mid H_r x \leq d_r \right\}, \quad r = 1,...N_r \tag{9}$$

and N_r denotes the total number of polyhedral regions in the partition. Algorithms for the construction of a polyhedral partition of the state space and computation of a PWA control law are given in (Maciejowski 2002, Cychowski 2009). In its simplest form, the PWA control law (8)–(9) can be evaluated by searching for a region containing current state x in its interior and applying the affine control law associated with this region. More efficient search strategies which offer a logarithmic-type complexity with respect to the total number of regions N_r in the partition have also been developed (Cychowski, 2009, Kvasnica et al. 2004, Tøndel et al. 2003, Spjøtvold et al. 2006). Nonetheless, the implementation of the explicit MPC control law can often be several orders of magnitude more efficient than solving the optimization problem (7) directly. This gain in efficiency is crucial for demanding applications with fast dynamics or high sampling rates in the milli/micro second range, such as the drive system considered in this paper.

4. MPC-based control structure

A typical electrical drive system is composed of a power converter-fed motor coupled to a mechanical system, a microprocessor-based controllers, current, rotor speed and/or position sensors used as feedback signals. Typically, cascade speed control structure containing two major control loops is used, as presented in Fig 2.
The inner control loop performs a motor torque regulation and consists of the power converter, electromagnetic part of the motor, current sensor and respective current or torque controller. As this control loop is designed to provide sufficiently fast torque control, it can be approximated by an equivalent first order term with small time constant. If the control is ensured, the driven machine could be an AC or DC motor, with no difference in the outer speed control loop. The outer loop consists of the mechanical part of the motor, speed sensor, speed controller, and is cascaded to the inner loop. It provides speed control according to the reference value (Szabat & Orlowska-Kowalska, 2007).
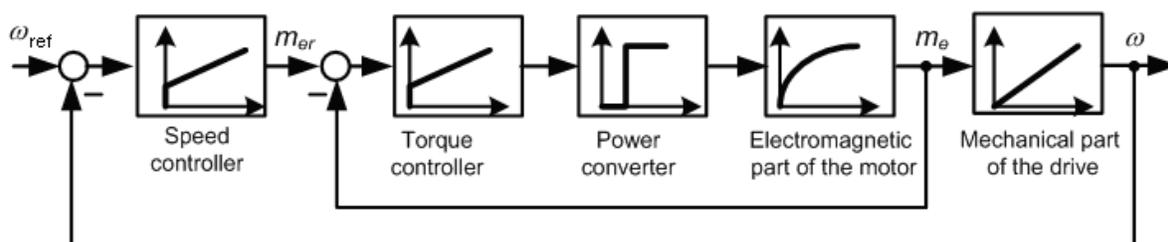

Fig. 2. The classical cascade control structure of the two-mass system

Such a classical structure in not effective enough in the case of the two-mass system. To improve the dynamical characteristics of the drive, the modification of the cascade structure is necessary. In this paper the structure with the MPC controller is considered which requires knowledge of all mechanical state variables of the drive. In the industrial applications, the direct measurement of the shaft torque m_s and the load speed ω_2 is very difficult. For that reason, in this paper the Kalman Filter (Szabat & Orlowska-Kowalska, 2008) is used to provide the information about non-measurable mechanical state variables. Additionally, the load torque m_L is also estimated and used in the MPC based control structure. In Fig. 3 the block diagram of the considered control structure is presented.
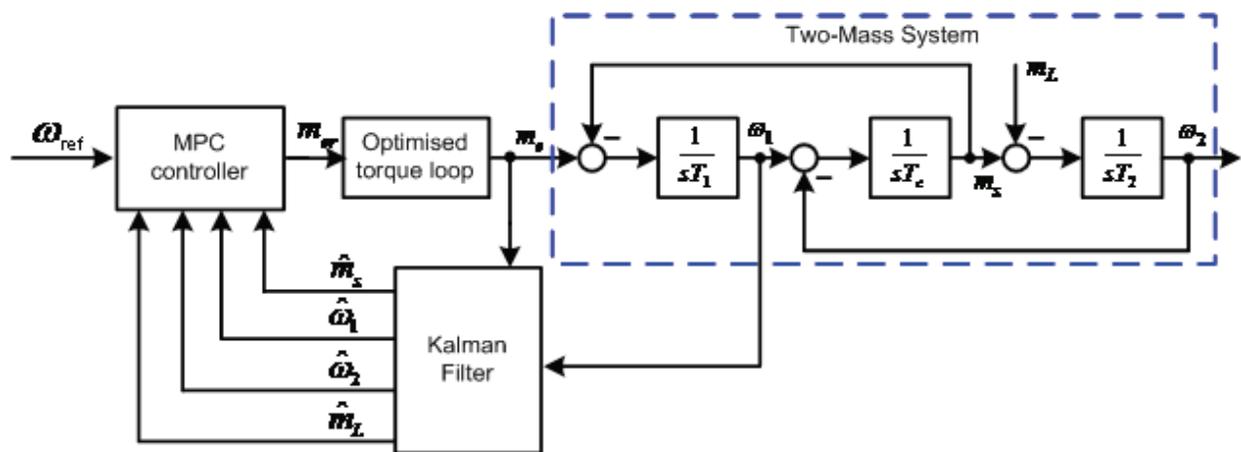
Fig. 3. The block diagram of the MPC-based control structure

5. Simulation study

In this section, the proposed single-loop explicit MPC control strategy for the drive system with an elastic coupling will be evaluated through simulations. A primary design objective for the MPC controller is to ensure that the load speed response follows the set-point with the desired dynamics. This needs to be achieved without generating excessive shaft torque responses and without violating the input and output constraints of the drive. The first two requirements can be addressed by defining the following auxiliary output variables:

$$y_1 = \omega_1 - \omega_{ref} \quad y_2 = \omega_2 - \omega_r \quad y_3 = m_s - m_L \tag{10}$$

where y_1 and y_2 account for tracking performance and y_3 relates to load-shaft torque imbalance. Due to (8)-(10), the reference speed variable and the disturbance torque need to be directly incorporated into the drive system model.

Decreasing the values of the cost function in the MPC algorithm leads to the minimization of the errors between the reference value of both speeds and reduce the torsional tension in the shaft. In order to calculate the values of the y_1-y_3, the original state vector of the system has to be extended by load torque m_L and the reference speed ω_r. Thus, the new model used in the MPC algorithm is described by the following state equation:

$$\frac{d}{dt}\begin{bmatrix} x_c \\ m_L \\ \omega_{ref} \end{bmatrix} = \begin{bmatrix} A_c & B_d & 0 \\ 0 & 0 & 0 \\ 0 & 0 & A_\omega \end{bmatrix} \cdot \begin{bmatrix} x_c \\ m_L \\ \omega_{ref} \end{bmatrix} + \begin{bmatrix} B_c \\ 0 \\ 0 \end{bmatrix} m_e \tag{11}$$

The dynamics of the reference value is described by the second order term:

$$G = \frac{\omega_o^2}{s^2 + 2\varsigma\omega_o s + \omega_o^2} \tag{12}$$

where ω_o is a reference frequency and the ς is the damping coefficient of the reference model.

The task of the MPC controller is to bring the output variables to zero by manipulating m_{er} while respecting the safety and physical limitations of the drive system, which in the analysed case are set as follows:

$$-3 \le m_{er} \le 3 \quad -1.5 \le m_s \le 1.5 \tag{13}$$

The selection of the prediction and control horizons is a compromise between the drive performance and computational complexity. In practice, $N_c \le N_p$ to avoid large computational burden for the standard MPC and large number of regions for the explicit MPC.

The dynamic of the control system with MPC controller can be adjusted by the changes of the values of the **Q** matrix. In the current work only the elements located in the main diagonal of the matrix have been changed. The form of the matrix **Q** used in the study is presented below:

$$\mathbf{Q} = \begin{bmatrix} q_{11} & 0 & 0 \\ 0 & q_{22} & 0 \\ 0 & 0 & q_{33} \end{bmatrix} \tag{14}$$

Taking into account (10) and (14) the cost function can be presented as follows:

$$J = \sum_{p=1}^{N} \left(q_{11} \left(\omega_1(p) - \omega_{ref}(p) \right)^2 + q_{22} \left(\omega_2(p) - \omega_{ref}(p) \right)^2 + q_{33} \left(m_s(p) - m_L(p) \right)^2 \right) + \sum_{k=0}^{N_u-1} \left(r \cdot m_e(k)^2 \right) \tag{15}$$

The robustness of the MPC algorithm is ensured by the suitable selection of the elements of matrix in (14) with the help of the pattern search algorithm. The cost function used in the optimization algorithm is as follows:

$$F = \min_{q_{11}; q_{22}; q_{33}} \left[\prod_{i=1}^{3} \left(f_i \left(e_1, e_2, e_3, K_1, K_2 \right) \right) \cdot f_4(e_4) \right] \tag{16}$$

where: e_1- tracking terror of motor speed ω_1, e_2- tracking terror of load speed ω_2, K_1 – penalty coefficient for exceeds of the limit of the shaft torque, K_2 - penalty coefficient for overshoot in the load speed, e_3 – coefficient in the cost function responsible for minimization of the tracking error of the speed for the systems with a different value of the parameter T_2. The terms of the (16) can be represented as in (17):

$$f_1^{T_2=T_{2N}} = \left\{ \sum_1^n \left(\left| \omega_{ref} - \omega_1 \right| \right) + \sum_1^n \left(\left| \omega_{ref} - \omega_2 \right| \right) + K_1 + K_2 \right\}$$

$$f_1^{T_2=0.5 \cdot T_{2N}} = \left\{ \sum_1^n \left(\left| \omega_{ref} - \omega_1 \right| \right) + \sum_1^n \left(\left| \omega_{ref} - \omega_2 \right| \right) + K_1 + K_2 \right\}$$

$$f_1^{T_2=2 \cdot T_{2N}} = \left\{ \sum_1^n \left(\left| \omega_{ref} - \omega_1 \right| \right) + \sum_1^n \left(\left| \omega_{ref} - \omega_2 \right| \right) + K_1 + K_2 \right\} \tag{17}$$

$$f_4 = \left\{ \sum_1^n \left(\left| \omega_2^{T_2=T_{2N}} - \omega_2^{T_2=0.5T_{2N}} \right| \right) + \sum_1^n \left(\left| \omega_2^{T_2=T_{2N}} - \omega_2^{T_2=2T_{2N}} \right| \right) \right\}$$

Penalty coefficient K_1 and K_2 can be expressed as (18):

$$K_1 = \begin{cases} 0 \Rightarrow for\ m_s \le m_s^{\max} \\ k_1 \cdot \left(m_s - m_s^{\max}\right) \Rightarrow for\ m_s > m_s^{\max} \end{cases}$$

$$K_2 = \begin{cases} 0 \Rightarrow for\ \omega_2 \le \omega_2^{ref} \\ k_2 \cdot \left(\omega_2 - \omega_2^{ref}\right) \Rightarrow for\ \omega_2 > \omega_2^{ref} \end{cases} \tag{18}$$

The responses of the reference model used under simulation study are shown in Fig. 4.
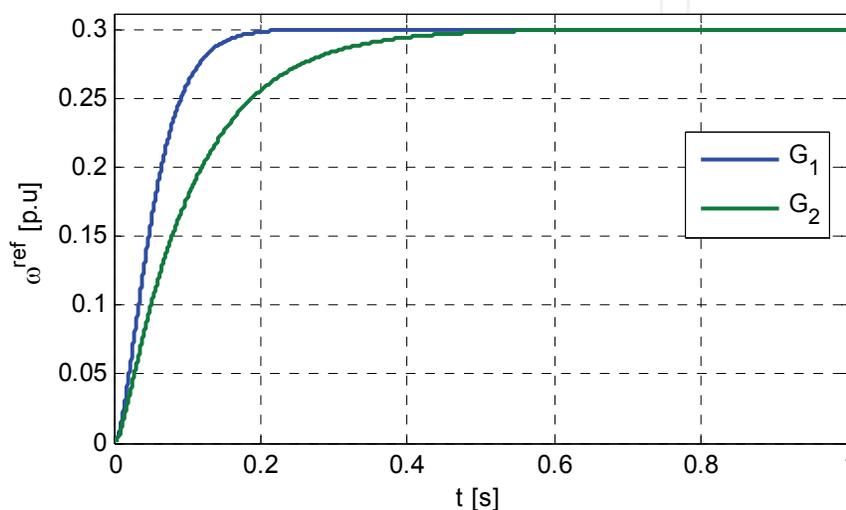
Fig. 4. The responses of the reference models used in the study

As can be concluded from Fig. 4, the settling times for the utilized reference models are 0.2 and 0.4s. These transients determine responses of the system. The pattern search algorithm is looking a one set of values in the matrix **Q** which enables the smallest difference between the speeds and the reference value for different value of the time constant of the load machine. The optimization algorithm has been working with the set value of the reference signal equal to 0.25 of the nominal speed in order to avoid the electromagnetic torque limit.

Transients of the state variables of the system working with the MPC algorithm for slower reference model are presented in Fig.5 . The parameters of the MPC controller are as follows: N=12, N_u=2, numbers of the regions: 121, while values in the matrix are diag(**Q**) = [8.89 0.15 198.2]. The value of cost function in pattern search algorithm is F=1.22e-7.

As can be concluded from the transients presented in Fig. 5, the system is working correctly. The load speed transients for different value of the load side inertia are close to the reference signal. The difference between the motor speed and the reference signal is slightly bigger than – between the reference and the load speed (which comes from the small value of the q_{11}). The application of the load torque causes the speed drop which is eliminated quickly. Those drop is bigger for the system with the smaller value of the load inertia significantly. During this disturbance the electromagnetic torque as well as the shaft torque reach the maximal allowed value for those states. In Fig. 5e the enlarged transients of the load speed errors are presented. It is clearly visible that during the start-up the drive with the biggest inertia has the biggest error.

In the work, a system with increased length of the control horizon has been investigated also. The increase of N_u from 2 to 3 allows to reduce the value of the cost function to 6.78e-8. However, at the same time the number of the controller regions goes up to 381. Due to the large computational complexity (significant in the experiment) the result related to this controller are not presented.

Next the system with faster reference model has been tested. After the optimization procedure the following values of the matrix **Q** were set: diag(**Q**)= [17.22 0.40 398.15]. The transients of the tested system are presented in Fig.6.

The drive systems with different inertia ratio have correct properties. The load speed transients cover the reference value almost perfectly. A much bigger difference exists in the transients of the motor speed. It comes from the small value of q_{11}, as in the previous case. The torsional vibrations are not evident in the system transients. The biggest value of the electromagnetic as well as the shaft torque characterise the system with the biggest inertia. The application of the load torque causes the speed drop but the reaction of the system to the disturbance is very dynamic. The electromagnetic torque reaches its allowed limit (Fig. 6a) in a short while.
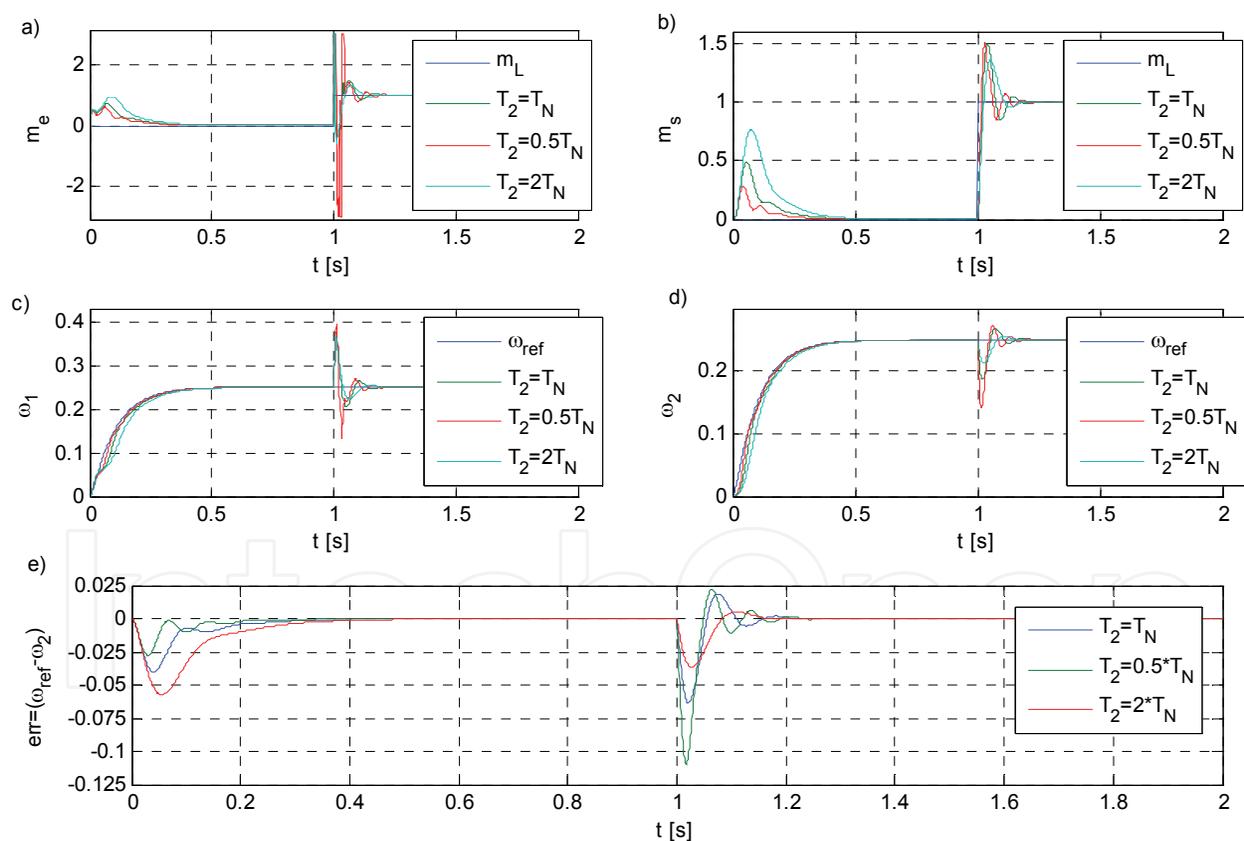

Fig. 5. Transients of the drive system: electromagnetic torque (a), shaft torque (b), motor speed (c), load speed (d), load speed errors (e) for the system with slower reference model and the controller parameters N=12, N_u=2

Finally, the system has been investigated for a bigger value of the reference speed and slower reference model. The values of the parameters of the matrix **Q** remain unchanged

(the same as for the ω_{ref}=0.25). The transients of the state variables of the system are presented in Fig. 7.

As can be seen from Fig. 7, the increase of the value of the reference speed changes the working point of the drive. During the start-up the electromagnetic torque is limited in all cases. Because of this limitation the speeds of the drive cannot follow the reference value. The bigger error appears in the system with T_2=2*T_2 due to the biggest inertia value of the entire drive system. What is evident from the shaft torque transients is that its limitations are in general prevented. Some small exceeds, which come from the applied softening strategy, are visible. However, they are eliminated fast.
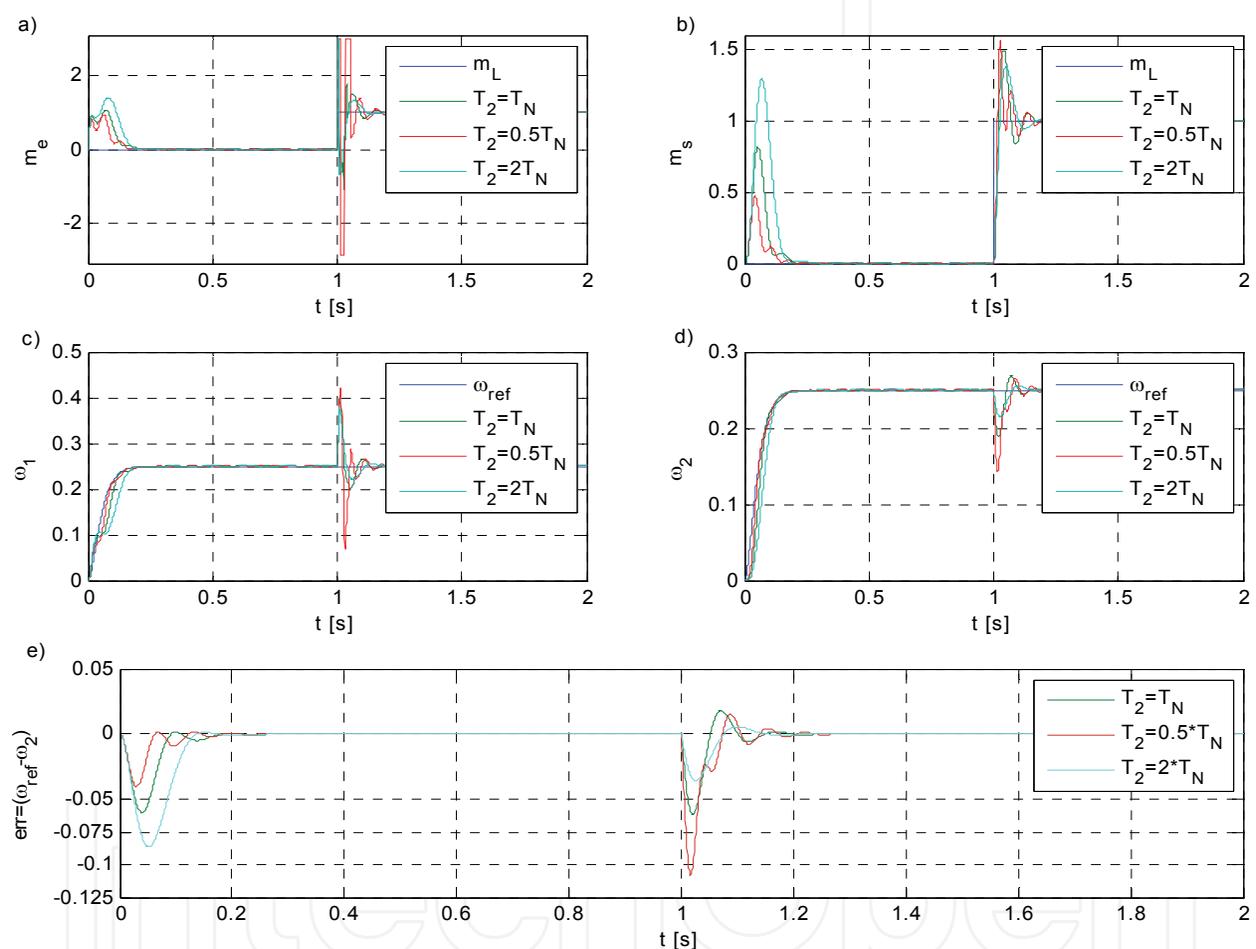

Fig. 6. Transients of the drive system: electromagnetic torque (a), shaft torque (b), motor speed (c), load speed (d), load speed errors (e) for the system with faster reference model and the controller parameters N=12, N_u=2

The pattern search algorithm is not robust against local minimum. In order to eliminate this drawback the starting point of the algorithm has been selected many times. The best three solutions obtained for the three different starting points v_1=[100 100 100]; v_2=[10 10 10]; v_3=[0.1 0.1 0.1] are presented in Tab. 1.

Despite the fact that the value of the cost function is similar for three starting values, the finding points are different. However, the ratios between find values are similar in every

case. It confirms that the find solution is the global solution or very close to it. The parameters of the optimization procedure are presented in Fig. 8.

V	Iteration	F	Finding points		
v_1	57	7.8784e-08	9188	184.0429	206948
v_2	51	7.9072e-08	930	24.1264	21898
v_3	60	8.7297e-08	17.2250	0.4017	398.10

Table 1. Parameters related to the pattern search algorithm
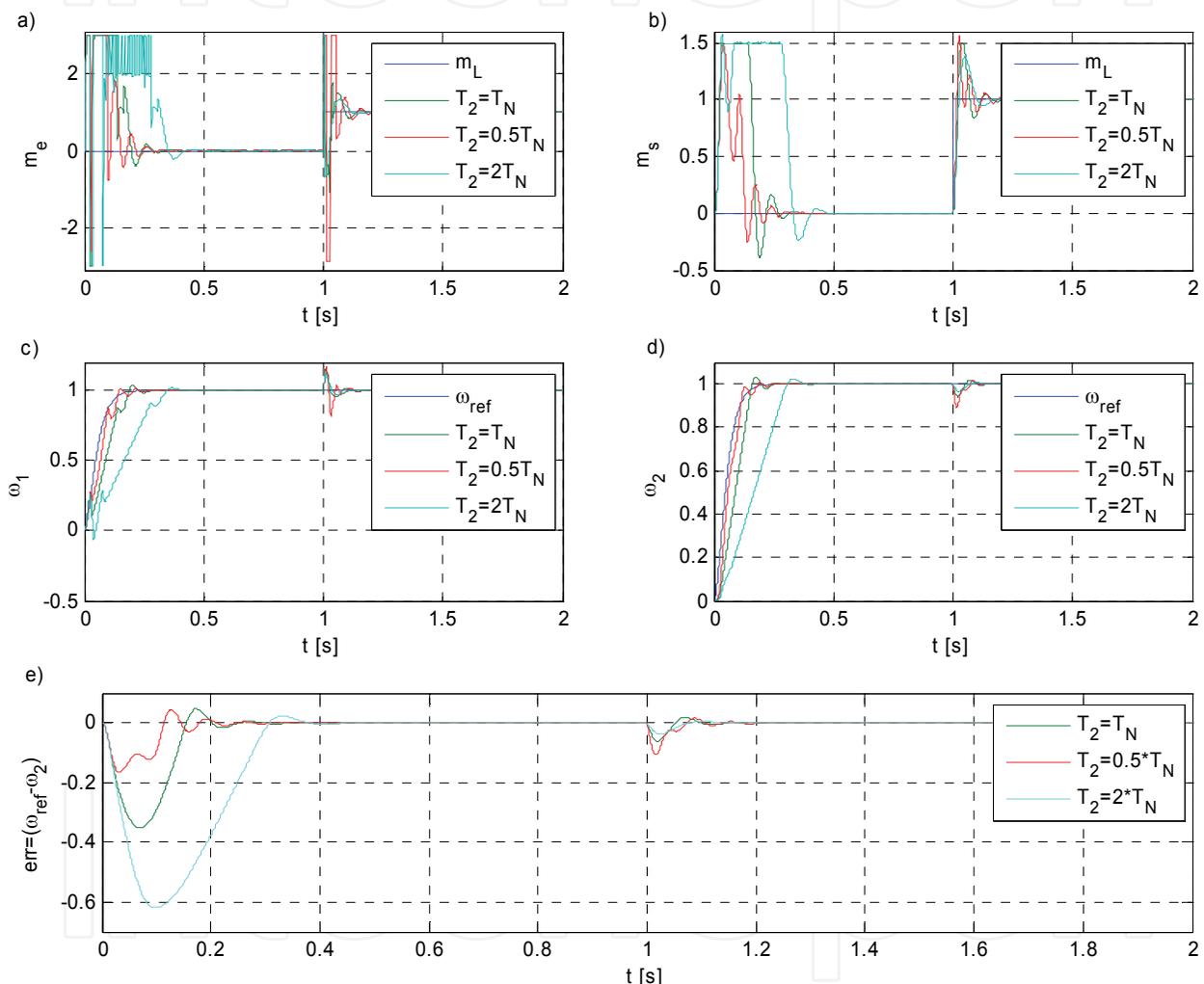
Fig. 7. Transients of the drive system: electromagnetic torque (a), shaft torque (b), motor speed (c), load speed (d), load speed errors (e) for the system with faster reference model and the controller parameters N=12, N_u=2 and nominal value of the reference speed

6. Experimental results

All theoretical considerations have been confirmed experimentally in a laboratory set-up composed of a 0.5kW DC-motor driven by a static converter. The motor is coupled to a load machine by an elastic shaft (a steel shaft of 5mm diameter and 600mm length). The speed

and position of the driven and loading motors have been measured by incremental encoders (36000 pulses per rotation). The mechanical system has a natural frequency of approximately 9.5Hz, while the nominal parameters of the system are T_1=203ms, T_2=203ms, T_c=2.6ms. The picture of the experimental set-up is presented in Fig. 9.

The control structure of the drive is shown in Fig. 3. The sampling time of the electromagnetic torque control as well as the estimator is 100μs in the experimental system. The outer speed control loop has the sampling time equal to 500 μs.
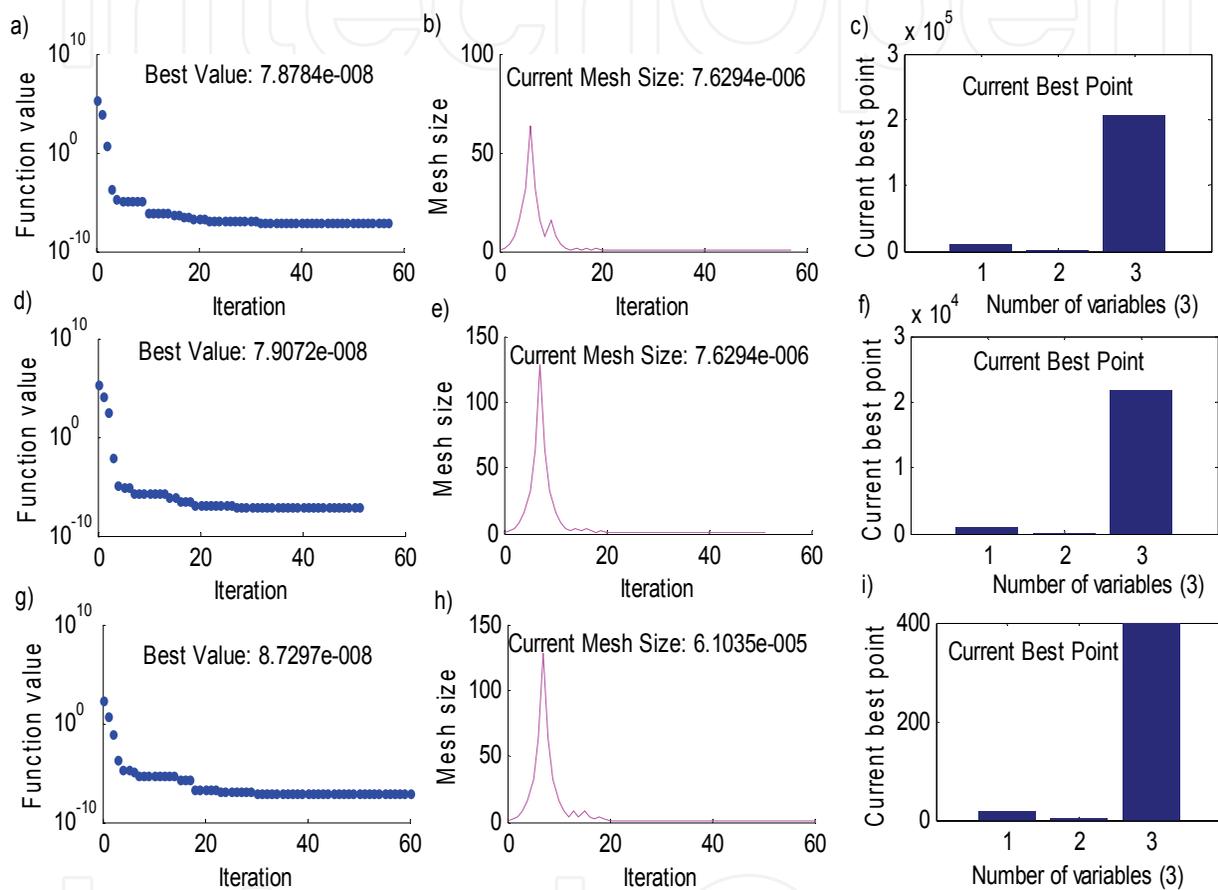
Fig. 8. The parameters of the pattern search algorithm: variation of the cost function (a,d,g), variation of the grid (b,e,h), found values of the parameters (c,f,i) for starting point v1 (a,b,c), v2 (d,e,f), v3 (g,h,i)

In the experimental study the system with a slower reference model has been tested. In Fig. 10 the transients of the motor speeds (a), shaft torques (b), load speed (c) as well as the tracking errors (c) for the drive system with nominal and twice bigger value of the load side inertia are presented. The system was tested for two inertia values of the loading machine.

As can be concluded from the presented transients the drive system works correctly. The shape of the load speeds obtained for different inertia ratio almost perfectly covers the transients of the reference model (Fig. 10). Also the tracking errors between the motor speeds and the reference model are very small. Similarly as in the simulation study, the tracking error during the start-up is bigger for the system with a bigger value of inertia (Fig. 10d). Contrary to this situation, the application of the load torque causes the bigger tracking

error in the system with smaller inertia. The transients of the shaft torque are presented in Fig. 10b. There are no limit exceeds in the shaft torque.

a)   b)
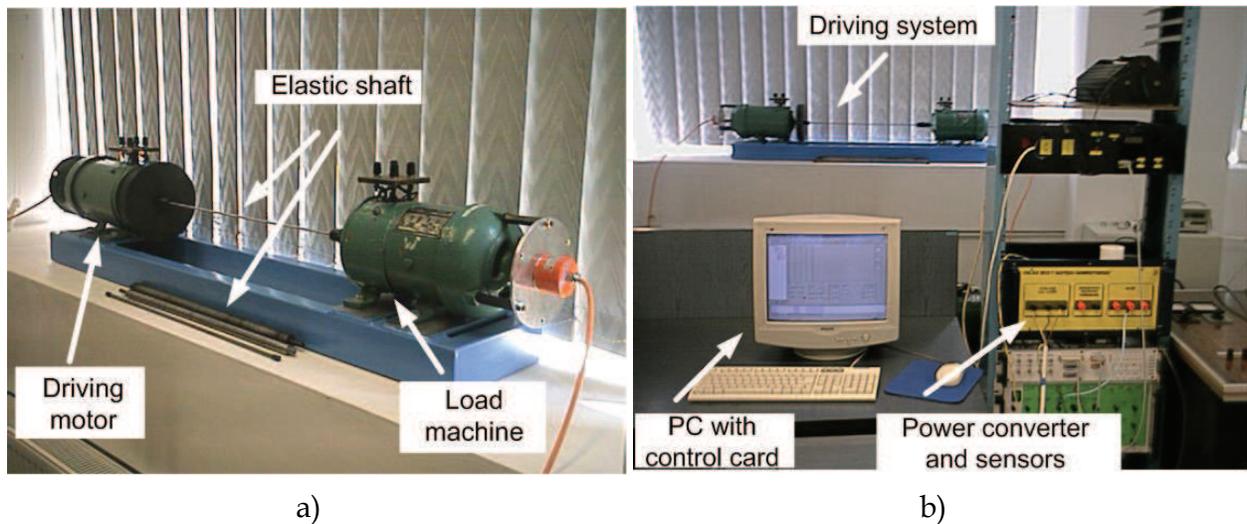
Fig. 9. The mechanical part of the laboratory set-up (a) and the general view of the laboratory set-up (b)
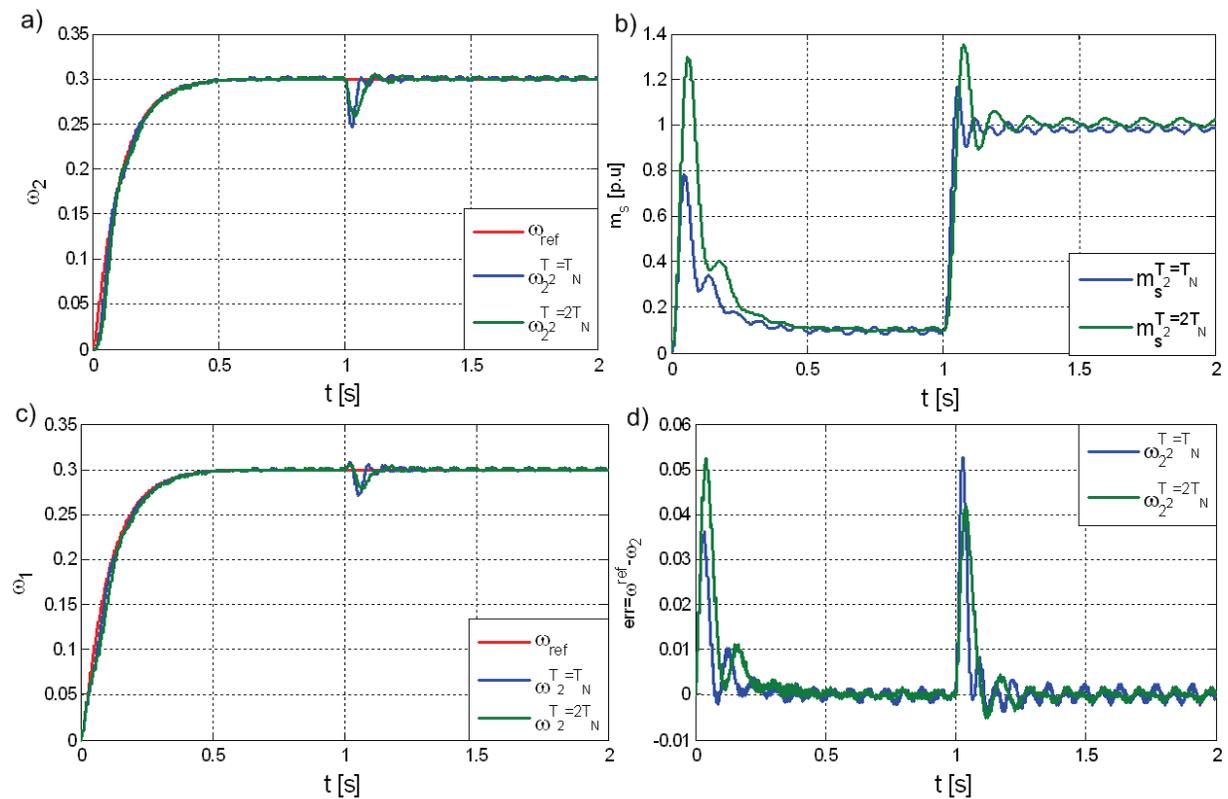
Fig. 10. Transients of the drive system: electromagnetic torque (a), shaft torque (b), motor speed (c), load speed (d), load speed errors (e) for the system with slower reference model and value of the reference speed ω_{ref}=0.25.

After the experiment presented above the system has been examined for nominal value of the reference speed. The drive transients are presented in Fig. 11. As in the previous case, the drive system is working in a stable way. For nominal parameters the motor and the load speeds follow the reference value without noticeable errors (Fig. 11a, c). It steams from the fact that the shaft torque reaches its maximal limits only for a short time (Fig. 11b). During this time the tracking error increases. Then, when the system is below the limit the tracking error goes to zero. The transients of speeds for the system with a bigger value of inertia do not follow the reference value during the start-up because of the limitation of the electromagnetic and shaft torque set in the system. Enlarging the value of these limits will allow to follow the reference system without the error. However, at the same time the mechanical stress could damage the whole drive system.
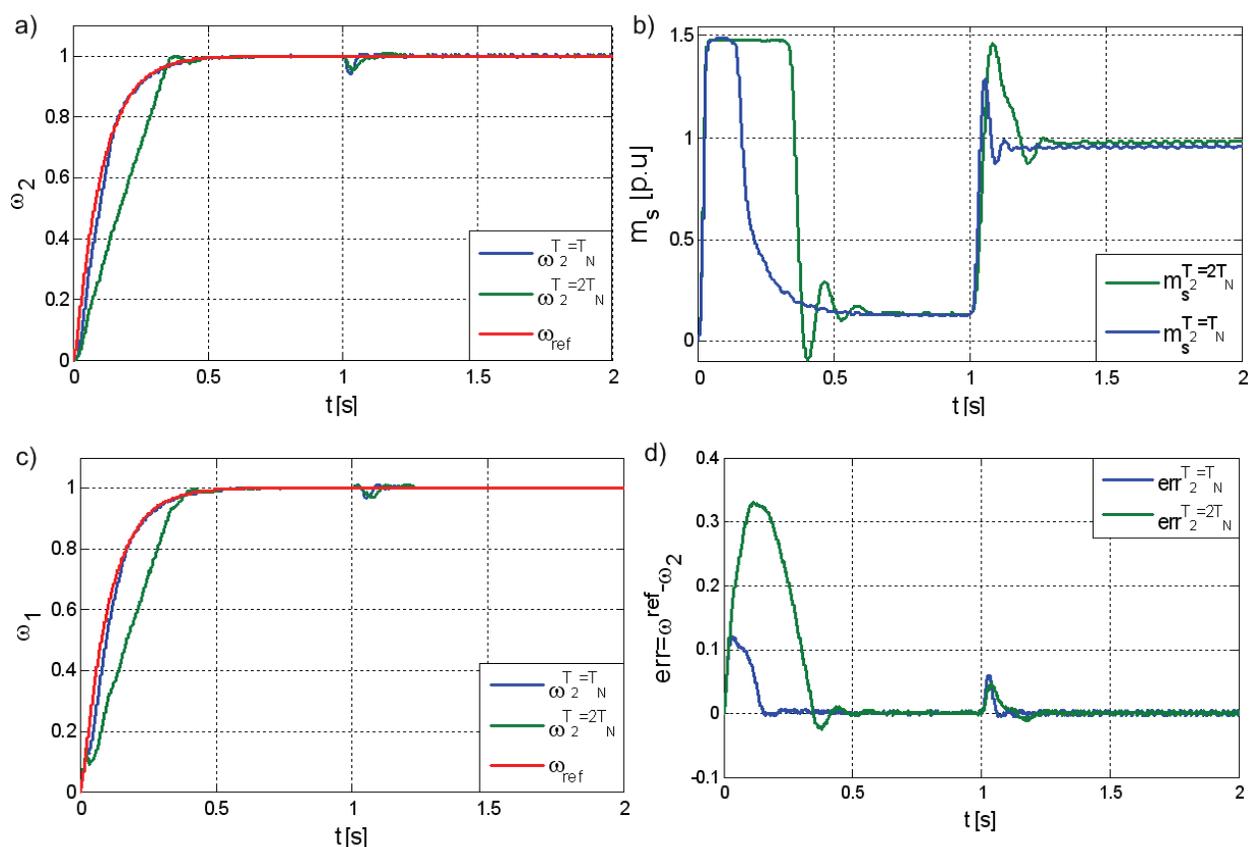

Fig. 11. Transients of the drive system: electromagnetic torque (a), shaft torque (b), motor speed (c), load speed (d), load speed errors (e) for the system with slower reference model and value of the reference speed w_r=0.25.

7. Conclusion

In order to damp the torsional vibrations, which could destroy the mechanical coupling between the driven and loading machine, the control structure with MPC is applied. The coefficients used in MPC are set using the optimization method in order to make the system robust against the changes of the load side inertia. The constraints of the electromagnetic and shaft torques are included during the design of the control algorithm.

As can be concluded from the presented results, the drive system works correctly despite parameter variations. The set control constraints of the shaft torque are not validated. It means that the control structure based on the MPC can ensure safe work in a drive system with uncertain or changeable parameters.

The future work will be devoted to designing of an adaptive MPC control. A part of its work will be the design methodology of a robust Kalman filter used to estimate the mechanical parameters of the drive.

8. Acknowledgements

9. References

Cychowski, M. T. (2009). Robust Model Predictive Control, *VDM Verlag*.

Cychowski, M.T., Szabat, K. & Orlowska-Kowalska T., (2009). Constrained Model Predictive Control of the Drive System with Mechanical Elasticity, *IEEE Trans. Ind. Electronics*, Vol. 56, No. 6, pp 1963-1973.

Erbatur, K., Kaynak, O. & Sabanovic A. (1999). A Study on Robustness Property of Sliding Mode Controllers: A Novel Design and Experimental Investigations, *IEEE Transaction on Industrial Electronics*, Vol. 46, No. 5, pp. 1012-1018.

Erenturk, K. (2008). Nonlinear two-mass system control with sliding-mode and optimised proportional and integral derivative controller combined with a grey estimator, *Control Theory & Applications, IET*, Vol. 2, No. 7, pp. 635 – 642.

Ferretti, G., Magnoni, G. A., Rocco, P., Vigano, L. & Rusconi, A. (2005). On the Use of Torque Sensors in a Space Robotics Application,: *Proc. on the IEEE/RSJ International Conference on Intelligent Robots and Systems IROS 2005*, pp. 1947- 1952, Canada.

Gu D. W., Petkov P. H., Konstantinov M. M. (2005). Robust Control Design with Matlab®, *Springer*.

Hace. A., Jezernik, K. & Sabanovic, A. (2005). Improved Design of VSS Controller for a Linear Belt-Driven Servomechanism, *IEEE/ASME Trans. on Mechatronics*, Vol. 10, No. 4, pp. 385-390.

Hirovonen, M., Pyrhonen, O. & Handroos H. (2006). Adaptive nonlinear velocity controller for a flexible mechanism of a linear motor, Mechatronic, *Elsevier*, Vol. 16, No. 5, pp. 279-290.

Hori, Y., Sawada, H. & Chun, Y. (1999). Slow resonance ratio control for vibration suppression and disturbance rejection in torsional system, *IEEE Trans. on Industrial Electronics*, Vol. 46, No. 1, pp. 162-168.

Itoh D., Iwasaki M., Matsui N. (2004). Optimal Design of Robust Vibration Suppression Controller Using Genetic Algorithms, *IEEE Transaction on Industrial Electronics*, Vol. 51, No. 5, pp. 947-953.

Ji, J. K. & Sul, S. K. (1995). Kalman Filter and LQ Based Speed Controller for Torsional Vibration Suppression in a 2-Mass Motor Drive System, *IEEE Trans. on Industrial Electronics*, Vol. 42, No. 6, pp. 564-571.

Kvasnica, M., Grieder, P., Baotic, M. & Morari, M., (2004) Multi-Parametric Toolbox (MPT), HSCC (Hybrid Systems: Computation and Control), Lecture Notes in Computer Science, Vol. 2993, pp. 448-46.

Kennel, R., Kazmierkowski, M.P., Rodriguez, J. & Cortes, P., (2008). Predictive Control in Power Electronics and Drives, *Tutorial in Int. Symp. on Industrial Electronics*, Cambridge, UK.

Maciejowski J.M. (2002). Predictive Control with Constraints, *Prentice Hall*, UK.

Michels, K., Klawonn, F., Kruse, R. & Nürnberger, A. (2006). Fuzzy Control – Fundamentals, Stability and Design of Fuzzy Controllers, *Springer*.

Orlowska-Kowalska, T. & Szabat, K. (2008). Damping of Torsional Vibrations in Two-Mass System Using Adaptive Sliding Neuro-Fuzzy Approach, *IEEE Transactions on Industrial Informatics*, Vol. 4, No. 1, pp. 47-57.

O'Sullivan, T., Bingham, C. C. & Schofield, N. (2007), Enhanced Servo-Control Performance of Dual-Mass System, *IEEE Trans. on Ind. Electronics*, Vol. 54, No. 3, pp. 1387-1398.

Qiao, R., Zhu, Q. M., Li, S. Y. & Winfield, A. (2002). Torsional Vibration Suppression of a 2-Mass Main Drive System of Rolling Mill with KF Enhanced Pole Placement, *Proc. of the 4th World Congress on Intelligent Control and Automation*, pp. 206-210, China.

Sugiura, K. & Hori, Y. (1996). Vibration Suppression in 2- and 3-Mass System Based on the Feedback of Imperfect Derivative of the Estimated Torsional Torque, *IEEE Trans. on Industrial Electronics,* Vol. 43, No. 2, pp. 56-64.

Suh, G., Hyun, D. S., Park, J. I., Lee, K. D. & Lee, S. G. (2001), Design of a Pole Placement Controller for Reducing Oscillation and Settling Time in a Two-Inertia System, *Proc. of 24th Annual Conference of the IEEE Industrial Electronics Society IECON'01,* pp. 1439-1444, USA.

Szabat, K. & Orłowska-Kowalska, T. (2007). Vibration Suppression in Two-Mass Drive System using PI Speed Controller and Additional Feedbacks – Comparative Study, *IEEE Trans. on Industrial Electronics,* Vol. 54, No. 2, pp.1193-1206.

Szabat, K. & Orlowska-Kowalska, T. (2008). Performance Improvement of Industrial Drives With Mechanical Elasticity Using Nonlinear Adaptive Kalman Filter, *IEEE Transactions on Industrial Electronics*, Vol. 55, No. 3, pp. 1075-1084.

Ryvkin, S., Izosimov, D. & Bayda, S. (2003). Flex mechanical digital control design, *Proceedings of IEEE International Conference on Industrial Technology, IEEE ICIT'03*, Vol.1, pp. 298-302.

Spjøtvold, J., Kerrigan, E.C., Jones, C.N., Tøndel, P., & Johansen, T.A. (2006). On the facet-to-facet property of solutions to convex parametric quadratic programs, *Automatica*, Vol. 42, No. 12, pp. 2209-2214.

Tøndel, P., Johansen, T.A., & Bemporad, A. (2003) An algorithm for multi-parametric quadratic programming and explicit MPC solutions, *Automatica*, Vol. 39, No. 3, pp. 489-497.

Vasak M. & Peric N., (2009), Stability analysis of a patched LQR control system for constrained multi-mass electrical drives, *Przeglad Elektrotechniczny*, Vol. 85, No. 7, pp. 109–114.

Vukosovic, S., N. & Stojic, M. R., (1998). Suppression of Torsional Oscillations in a High-Performance Speed Servo Drive, *IEEE Trans. on Industrial Electronic*, Vol. 45, No. 1, pp. 108-117.

Wang L., Frayman Y. (2002). A Dynamically Generated Fuzzy Neural Network and its Application to Torsional Vibration Control of Tandem Cold Rolling Mill Spindles, *Engineering Applications of Artificial Intelligence,* Vol.15, No. 6, pp. 541-550.
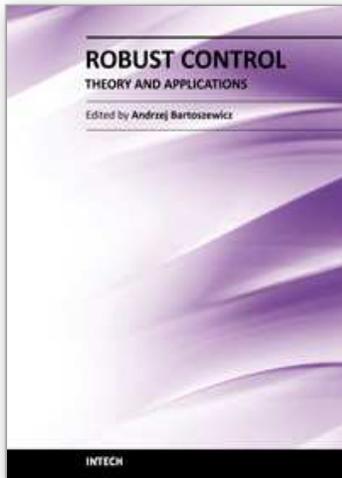
Robust Control, Theory and Applications

Edited by Prof. Andrzej Bartoszewicz

The main objective of this monograph is to present a broad range of well worked out, recent theoretical and application studies in the field of robust control system analysis and design. The contributions presented here include but are not limited to robust PID, H-infinity, sliding mode, fault tolerant, fuzzy and QFT based control systems. They advance the current progress in the field, and motivate and encourage new ideas and solutions in the robust control area.

How to reference

In order to correctly reference this scholarly work, feel free to copy and paste the following:

Krzysztof Szabat, Teresa Orłowska-Kowalska and Piotr Serkies (2011). Robust Control of the Two-mass Drive System Using Model Predictive Control, Robust Control, Theory and Applications, Prof. Andrzej Bartoszewicz (Ed.), ISBN: 978-953-307-229-6, InTech, Available from: http://www.intechopen.com/books/robust-control-theory-and-applications/robust-control-of-the-two-mass-drive-system-using-model-predictive-control

INTECH
open science | open minds